

Magnetic properties of $\text{La}(\text{Fe}_x\text{Al}_{1-x})_{13}$ determined via neutron scattering and Mössbauer spectroscopy

R. B. Helmholdt

Energieonderzoek Centrum Nederland ECN, NL-1755 ZG Petten, The Netherlands

T. T. M. Palstra, G. J. Nieuwenhuys, and J. A. Mydosh

Kamerlingh Onnes Laboratorium der Rijksuniversiteit Leiden, Postbus 9506, NL-2300 RA Leiden, The Netherlands

A. M. van der Kraan

Interuniversitair Reactor Instituut, NL-2629 JB Delft, The Netherlands

K. H. J. Buschow

Philips Research Laboratories, Postbus 80 000, NL-5600 JA Eindhoven, The Netherlands

(Received 26 August 1985)

$\text{La}(\text{Fe}_x\text{Al}_{1-x})_{13}$ pseudobinary intermetallic compounds, which can be stabilized for $0.46 < x < 0.92$, have been studied by neutron diffraction and Mössbauer spectroscopy. Neutron measurements on an antiferromagnetic $x = 0.91$ sample at 4.2 K reveal a long-range-order antiferromagnetic state, consisting of ferromagnetic clusters, coupled antiferromagnetically. Mössbauer-effect measurements show a drop of the hyperfine field at the Fe nucleus at the ferromagnetic-antiferromagnetic phase boundary $x \approx 0.88$. Both these microscopic measurements indicate a transition from α -iron-like ferromagnetism to γ -iron-like antiferromagnetism due to the extremely high coordination of Fe atoms.

I. INTRODUCTION

$\text{La}(\text{Fe}_x\text{Al}_{1-x})_{13}$ intermetallic compounds exhibit a unique magnetic phase diagram, although they can only be stabilized in the x range between 0.46 and 0.92 (Ref. 1). At these x values the structure is not stable with respect to LaFe_4Al_8 and pure α -Fe. In spite of its limited composition range, this system exhibits three different types of magnetic order: (i) at low iron concentration a mictomagnetic state was found, originating from a competition between antiferromagnetic Fe-Al-Fe superexchange and ferromagnetic Fe-Fe direct exchange, (ii) at higher iron concentrations a soft ferromagnetic state exists, and finally, (iii) at the highest iron concentrations an antiferromagnetic state was observed. In the ferromagnetic regime magnetization experiments showed that the Fe moment follows the Slater-Pauling curve. Mössbauer measurements revealed a hyperfine field at the Fe nucleus proportional to the saturation moment, with a proportionality constant of about $14 \text{ T}/\mu_B$, in agreement with other Fe-based intermetallics.^{2,3}

In contrast to this normal behavior, the antiferromagnetic regime displays sharp metamagnetic transitions with large hysteresis effects in relatively low fields ($H \sim 5 \text{ T}$) compared to the transition temperature ($T \sim 200 \text{ K}$) (Ref. 4). The metamagnetic transitions are accompanied by large magnetostrictive effects ($\Delta V/V \sim 1\%$), which can be described via a combined band and local moment model.⁵ Also a large magnetoresistance effect ($\Delta\rho \sim 20 \mu\Omega \text{ cm}$) was observed at the metamagnetic transition and was discussed in terms of the two-spin current model.⁵

Despite this progress, the nature of the antiferromag-

netic structure is not immediately clear because no simple antiferromagnetic lattice can be mapped on the NaZn_{13} -type crystal structure due to the combined threefold and fourfold symmetry which always leads to frustration. Therefore, we have performed a neutron diffraction investigation to resolve the symmetry or frustration of the antiferromagnetic order. Additionally, Mössbauer spectroscopy measurements^{1,2} on this system have been extended into its antiferromagnetic state. Our measurements can be interpreted with a magnetic structure consisting of (1 0 0) planes with ferromagnetically coupled clusters with successive planes coupled antiferromagnetically. This is a unique structure for a system with only direct Fe-Fe magnetic interactions.

II. EXPERIMENTAL PROCEDURES

The $\text{La}(\text{Fe}_x\text{Al}_{1-x})_{13}$ samples were prepared by arc melting the appropriate amounts of starting materials in an atmosphere of ultra pure argon gas. The purity of the elements was better than 99.9%. After arc melting, the samples were vacuum annealed for about 10 days at 900°C . X-ray diffraction analysis showed that single-phase samples were obtained of the NaZn_{13} -type structure. However, neutron diffraction and Mössbauer spectroscopy showed that the samples are contaminated with several percents of α -Fe.

Neutron diffraction experiments at 4.2 and 300 K were performed on a ferromagnetic ($x = 0.69$) and an antiferromagnetic ($x = 0.91$) sample using the powder diffractometer at the High Flux Reactor (HFR) in Petten. Neutrons of wavelength $2.5913(4) \text{ \AA}$ were obtained after re-

flection from the (1 1 1) planes of a copper crystal. The λ/n contamination had been reduced to less than 0.1% using a pyrolytic graphite filter. Soller slits with a horizontal divergence of 30' were placed between the reactor and the monochromator and in front of the four ^3He counters. All data have been corrected for absorption, μR is 0.48 and 0.51 for $x=0.69$ and 0.91, respectively.

The ^{57}Fe Mössbauer spectra were obtained by means of a standard-constant-acceleration-type spectrometer in conjunction with a $^{57}\text{Co-Rh}$ source. The hyperfine fields were calibrated by means of the field in $\alpha\text{-Fe}_2\text{O}_3$ at 295 K (51.5 T). The isomer shift was measured relative to SNP at room temperature.

$\text{La}(\text{Fe}_x\text{Al}_{1-x})_{13}$ has the cubic NaZn_{13} structure, space group $\text{Fm}\bar{3}\text{c}$ (O_h^8). In the hypothetical compound LaFe_{13} the Fe atoms occupy two different sites, 8(b) and 96(i) for Fe^{I} and Fe^{II} , respectively. The La and the Fe^{I} atoms form a CsCl structure. The Fe^{I} atoms are surrounded by an icosahedron of twelve Fe^{II} atoms. The Fe^{II} icosahedra are packed in alternate directions so that one unit cell contains 8 icosahedra, and the lattice parameter is twice the $\text{Fe}^{\text{I}}\text{-Fe}^{\text{I}}$ distance. The Fe^{II} sites have 1 Fe^{I} and 9 Fe^{II} nearest neighbors. The shortest Fe-Fe distance is between the Fe^{I} and Fe^{II} being about 4% shorter than the $\text{Fe}^{\text{II}}\text{-Fe}^{\text{II}}$ distance. Note that this $\text{Fe}^{\text{I}}\text{-Fe}^{\text{II}}$ distance is about the same as for $\alpha\text{-Fe}$. Neutron diffractograms of two $\text{La}(\text{Fe}_x\text{Al}_{1-x})_{13}$ compounds, $x=0.69$ and 0.91, were measured at room temperature, well above the magnetic ordering temperatures, $T_C=237$ K and $T_N=218$ K, respectively, and at 4.2 K. The diffraction patterns were analyzed using Rietveld's refinement technique.⁶ All diffractograms are contaminated by the (1 1 0) and (2 0 0) peaks of $\alpha\text{-Fe}$, while the diffractograms at 4.2 K are contaminated also by two peaks due to the cryostat. The regions in which these two kinds of peaks occurred were excluded from the refinement.

III. EXPERIMENTAL RESULTS

The refinement analysis of the nuclear structure of the diffractograms at 300 K showed that the Fe^{I} sites in both compounds were predominantly (>97%) occupied by Fe. Thus the Al atoms are statistically distributed only over the 96(i) sites. The results for both the ferromagnetic ($x=0.69$) and antiferromagnetic ($x=0.91$) compound at 300 and 4.2 K are given in Table I. The calculated magnetic moment for the $x=0.69$ compound [$m=1.41(8)\mu_B/\text{Fe}$] is in agreement with the saturation moment $m=1.47(2)\mu_B/\text{Fe}$, measured previously.⁵

In the diffraction pattern of the $x=0.91$ compound extra peaks were found at 4.2 K with respect to that at 300 K (see Fig. 1). These extra peaks have mixed indices, whereas the nuclear peaks have indices all odd or all even. Hence, the compound has a long-range-ordered antiferromagnetic state and is not dominated by frustration effects as was inferred by an extremely high electrical resistivity of the antiferromagnetic state.⁵ Furthermore, this means that the magnetic unit cell coincides with the nuclear unit cell, which forms the basis of our cluster model (see below).

^{57}Fe Mössbauer spectra obtained at 4.2 K on various $\text{La}(\text{Fe}_x\text{Al}_{1-x})_{13}$ compounds are shown in Fig. 2. A decomposition of these spectra into subspectra associated with the Fe^{I} and Fe^{II} sites does not seem possible, owing to the fact that for both sites various types of nearest-neighbor coordinations exist, differing in the number and arrangement of nearest-neighbor Al atoms. Therefore we have restricted ourselves to determining only the average hyperfine field and isomer shift, which has been plotted as a function of concentration in Fig. 3. In this plot one recognizes the trend of the average hyperfine field to increase with x , the ferromagnetic-antiferromagnetic phase

TABLE I. Results from the final refinements for $\text{La}(\text{Fe}_x\text{Al}_{1-x})_{13}$. a is the lattice parameter, y and z are parameters of the NaZn_{13} -type crystal structure, d is the distance between Fe^{I} and Fe^{II} , \bar{B} the overall temperature factor, $m_{\text{Fe}^{\text{I}}}$ and $m_{\text{Fe}^{\text{II}}}$ the magnetic moment of Fe^{I} and Fe^{II} atoms, respectively, R_{nucl} and R_{magn} the reliability factor of the nuclear and magnetic structure, respectively, defined as $R = \Sigma |I(\text{obs}) - I(\text{calc})| / I(\text{calc})$ and χ^2_ν is defined as $\chi^2_\nu = \Sigma w_i [y_i(\text{obs}) - y_i(\text{calc})]^2 / \nu$, with $y_i(\text{obs})$ and $y_i(\text{calc})$ the observed and calculated values of the i th measuring point, w_i its statistical weight and ν the degrees of freedom.

	$x=0.69$		$x=0.91$	
	300 K	4.2 K	300 K	4.2 K
a (Å)	11.7378(3)	11.7235(3)	11.5788(3)	11.5932(3)
y	0.177 20(7)	0.177 38(6)	0.178 69(6)	0.179 38(6)
z	0.113 99(7)	0.113 69(7)	0.115 91(6)	0.116 24(7)
d (Å)	2.470	2.440	2.466	2.478
\bar{B} (Å ²)	0.64(5)	0.22(6)	0.61(5)	-0.04(5)
$M/\text{Fe-atom}$ (μ_B)		1.41(8)		2.05(3)
$M_{\text{Fe}^{\text{I}}}$ (μ_B)				1.10(7)
$M_{\text{Fe}^{\text{II}}}$ (μ_B)				2.14(3)
R_{nucl} (%)	2.2	1.8	1.3	1.3
R_{magn} (%)		3.0		21.4
χ^2_ν	13.0	6.8	8.6	5.1

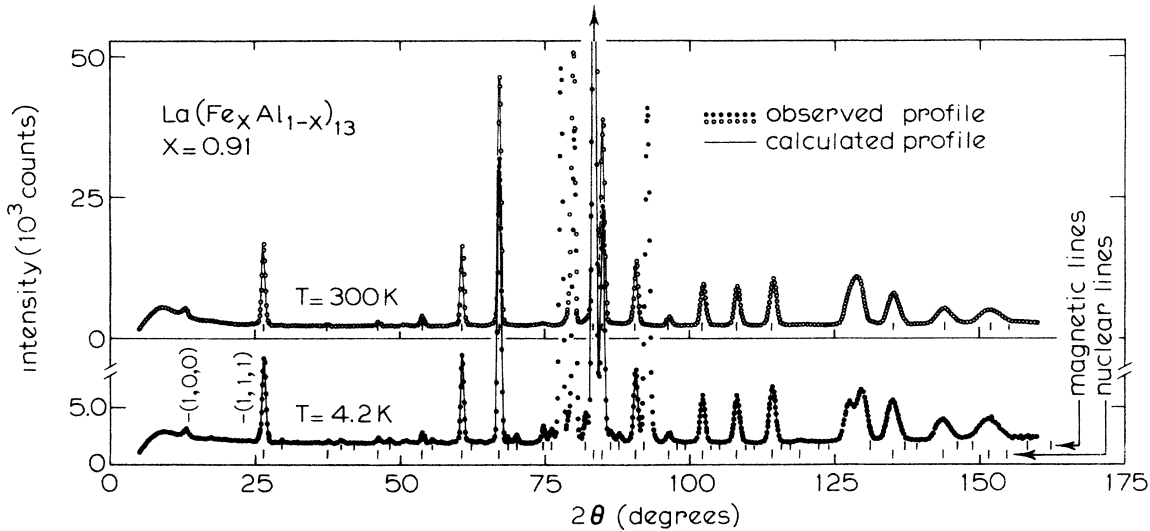


FIG. 1. Neutron powder diffractograms of $\text{La}(\text{Fe}_x\text{Al}_{1-x})_{13}$ with $x=0.91$ at 4.2 and 300 K. Both nuclear and magnetic lines are indicated. The drawn line through the data points is the calculated profile of the final refinement analysis.

boundary being revealed by a substantial drop of \bar{H}_{eff} close to $x=0.87$.

IV. DISCUSSION

As each unit cell of 8 formula units contains 104 spins, disregarding the presence of the Al atoms, it is impossible to resolve the magnetic structure without modeling the

system. Therefore the following simplifications have been made: (1) Each icosahedron of 12 Fe^{II} atoms together with the central Fe^{I} atom is considered as one entity or cluster. (2) The La and Al atoms are disregarded as they have no magnetic moment. (3) In addition, we assumed that the 12 Fe^{II} atoms of each cluster have their spins parallel, (4) while the central Fe^{I} atom of the cluster may have its spin either parallel or antiparallel to the surrounding spins. The spin of one cluster is represented by the resultant spin of the Fe spins constituting the cluster. For the $x=0.91$ sample this means that the cluster has a spin of $(13 \times 0.91 - 1)m(\text{Fe}^{\text{II}}) \pm m(\text{Fe}^{\text{I}})$. Thus, the problem of finding the magnetic structure of 104 spins in the unit cell has been reduced, i.e., simplified, to the magnetic structure of 8 cluster spins. This cluster assumption is the

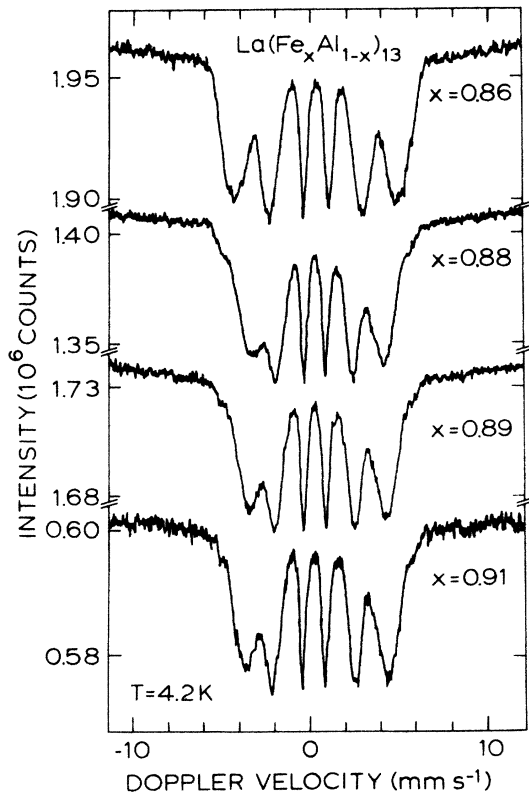


FIG. 2. ^{57}Fe Mössbauer spectra obtained at 4.2 K on various compounds of $\text{La}(\text{Fe}_x\text{Al}_{1-x})_{13}$.

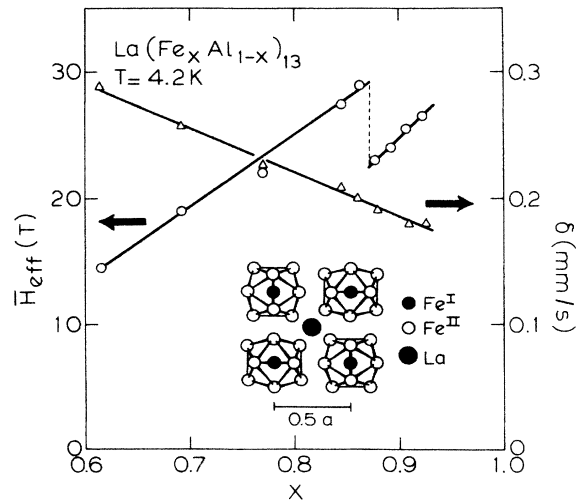


FIG. 3. Concentration dependence of the average hyperfine field \bar{H}_{eff} and the isomer shift δ in $\text{La}(\text{Fe}_x\text{Al}_{1-x})_{13}$ at 4.2 K. The inset shows a projection along the c axis of four Fe^{II} icosahedra plus central Fe^{I} atom (clusters).

only reasonable construction which avoids overlap of the clusters, since the next possible construction invokes 32 clusters. However, although these clusters do not overlap, one has to keep in mind that the Fe-Fe distances within a cluster are as large as between the clusters (see inset in Fig. 3). Four different antiferromagnetic structures were constructed and they are illustrated in Fig. 4. Models A, C, and D can be rejected because they require the distinct presence of the (1 0 0) and (1 1 1) reflections, which are definitely not present in the diffractogram at 4.2 K (see Fig. 1). Additionally, the refinement analysis of these models results in a magnetic reliability factor R_{magn} of 90–100%, which is considerably worse than $R_{\text{magn}} = 26\%$ for model B at the same stage of the refinement. Furthermore, the extinction conditions for the magnetic reflections of model B are not contradicted by our findings (h, k, l all mixed; $h + k = \text{even}$, $h + l = \text{odd}$, $k + l = \text{odd}$; all h, k, l with $h = \text{odd}$ or zero forbidden). Therefore, we conclude that model B represents best the magnetic structure. The best fit for model B is obtained with the central Fe^{I} spin *parallel* to the cluster spin and with a different Fe^{I} moment with respect to the surrounding Fe^{II} moments. Allowing the spins to make an angle with the z axis did not improve the fit. The final results of the refinement analysis are given in Table I. A magnetic moment of $2.14(3)\mu_B/\text{Fe-atom}$ for the Fe^{II} moment and $1.10(7)\mu_B/\text{Fe-atom}$ for the Fe^{I} moment has been obtained. From saturation magnetization experiments in a field beyond the spin-flip field (9.5 T), we found a value of $2.13(1)\mu_B/\text{Fe-atom}$ (Ref. 5). Hence the neutron measurements indicate that the Fe^{II} moments have no pronounced change of moment, going from the antiferromagnetic state to the field-induced state. However, they suggest that the Fe^{I} atoms do have a severe change of moment.

The Mössbauer spectra are less revealing in this respect, since they do not clearly show an additional spectral contribution in the antiferromagnetic state with a hyperfine field of about half the value, resulting from the reduced Fe^{I} moments. Such is not surprising since one has to take account of the fact that the additional spectrum would have only a relative intensity of 8%. In the second place, it cannot be excluded that there is a substantial change in the transferred hyperfine field, when changing from ferromagnetic to antiferromagnetic order. For the Fe^{I} and Fe^{II} moments this change may be of opposite sign, leading

to a decrease in the total hyperfine field for the Fe^{II} moments (see below), but to an increase for the Fe^{I} moments. Consequently, the corresponding two subspectra might not show a large difference in hyperfine field splitting at all, and the Fe^{I} subspectrum could be undetectable. As can be seen from Fig. 3, the drop in the mean effective hyperfine field at the magnetic phase boundary is not reflected in a jump in the isomer shift. This means that the s -electron density at the Fe nuclei does not change, which suggests that the drop in the mean effective hyperfine field is mainly associated with a change in magnitude and/or sign of the transferred hyperfine field when passing the magnetic phase boundary.

The model B we propose for the antiferromagnetic structure of $\text{La}(\text{Fe}_x\text{Al}_{1-x})_{13}$ may certainly not be interpreted as a determination of the exact magnitude and direction of each individual magnetic moment. This model is limited by the above assumptions of clusters and by the fact that we are treating a *pseudo*-binary compound leading to various surroundings of the Fe atoms by both Fe and Al atoms. Rather, magnitude and direction of the moments are determined by the local magnetic environment of each Fe moment, which may be concluded from the distribution of hyperfine fields in the Mössbauer measurements.² However, we think that our model reflects the basic symmetry of the magnetic order, in view of the rather good reliability factor R_{magn} , the fulfillment of the extinction conditions, and the occurrence of spin-flip transitions in relatively low magnetic fields (see below). This means that the magnitude of the moments as obtained from the refinement analysis ($2.14\mu_B/\text{Fe}$) must be considered as an averaged moment. However, as the magnetization also yields an averaged moment ($2.13\mu_B/\text{Fe}$), the excellent correspondence of the results further supports our model.

These results can be summarized as follows. We have found a new type of metamagnetic compound, where ferromagnetic (1 0 0) planes of clusters (icosahedra plus central atom) are formed and coupled antiferromagnetically. Therefore it is possible to spin flip the system in relatively low magnetic fields ($H < 15$ T) to an induced ferromagnetic state.⁴ The $\text{La}(\text{Fe},\text{Al})_{13}$ compound can thus be compared with other metamagnets with layered structures like Au_2Mn (Ref. 7), HoNi (Ref. 8), Pt_3Fe (Refs. 9 and 10), etc. Here there are also ferromagnetic interactions within a layer and antiferromagnetic interactions between the

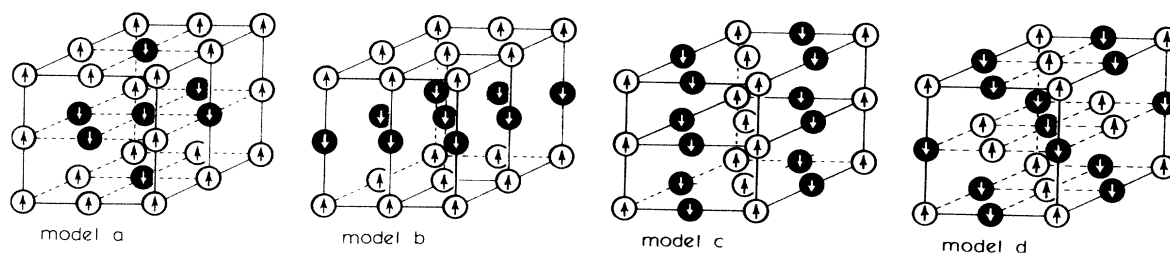


FIG. 4. The four models for the antiferromagnetic structure of $\text{La}(\text{Fe}_x\text{Al}_{1-x})_{13}$. Each spin represents the total spin of the cluster of thirteen atoms. The dashed lines are a guide to the eye, and the solid lines indicate the magnetic unit cell.

layers. However, for the latter compounds the layers are sheets of single atoms, whereas in $\text{La}(\text{Fe},\text{Al})_{13}$ the layers are planes of clusters. Furthermore, the layers in $\text{La}(\text{Fe},\text{Al})_{13}$ are not separated but directly adjacent to each other, whereas in compounds like Pt_3Fe and Au_2Mn the ferromagnetic layers are separated by another kind of atom, either magnetic or nonmagnetic.

The origin of the antiferromagnetic ground state of $\text{La}(\text{Fe},\text{Al})_{13}$ at high iron concentration is not clear at present. We believe that these antiferromagnetic interactions are crucially dependent on the local environment of the Fe atoms.^{11,12} At high Fe-Fe coordination numbers, up to 12 for Fe^{I} sites and up to 10 for Fe^{II} sites, an antiferromagnetic state can arise from the same causes as in the Invar alloys Fe-Ni (fcc) and Fe-Ni-Mn (fcc) and as in γ -Fe (fcc) (Refs. 13 and 14). This antiferromagnetic state was predicted for Fe-Ni, but was not found due to a martensitic crystallographic transition. However, it has indeed been found in Fe-Ni-Mn where the martensitic transition can be suppressed.¹⁵ Nevertheless, in this compound three magnetic constituents are present and hinder a straightforward interpretation. In contrast, for $\text{La}(\text{Fe},\text{Al})_{13}$ only the Fe-Fe exchange interactions have to be taken into account.

Finally, a confirmation of the reduction of the magnetic moments on the Fe^{I} atoms ($1.1\mu_B/\text{Fe}$) requires more specific information. No conclusive evidence can be obtained from our neutron measurements, unless the cluster assumption can be justified. Still, calculations of the magnitude of the Fe moment have indicated an instability of the magnetic moment in an fcc lattice, leading to a moment reduction.^{16,17} Thus, it was found that the Fe moment decreases with decreasing atomic radius of the Fe atom in an fcc lattice.¹⁷ In $\text{La}(\text{Fe},\text{Al})_{13}$ the Fe^{I} atoms have an fcc-like local environment and furthermore, the smallest atomic volume of the Fe atoms is found at the highest iron concentration, where the antiferromagnetic state arises.⁵ Hence, the moment reduction of the Fe^{I} atoms is likely to occur.

In conclusion, we have observed in $\text{La}(\text{Fe},\text{Al})_{13}$ a transition from a ferromagnetic α -Fe-like state to an antiferromagnetic γ -Fe-like state.

ACKNOWLEDGMENT

This work was supported in part by the Nederlandse Stichting voor Fundamenteel Onderzoek der Materie (FOM).

¹T. T. M. Palstra, J. A. Mydosh, G. J. Nieuwenhuys, A. M. van der Kraan, and K. H. J. Buschow, *J. Magn. Magn. Mater.* **36**, 290 (1983).

²A. M. van der Kraan, K. H. J. Buschow, and T. T. M. Palstra, *Hyperfine Interact.* **15/16**, 717 (1983).

³P. C. M. Gubbens, J. H. F. van Apeldoorn, A. M. van der Kraan, and K. H. J. Buschow, *J. Phys.* **4**, 921 (1974).

⁴T. T. M. Palstra, H. G. C. Werij, G. J. Nieuwenhuys, J. A. Mydosh, F. R. de Boer, and K. H. J. Buschow, *J. Phys. F* **14**, 1961 (1984).

⁵T. T. M. Palstra, G. J. Nieuwenhuys, J. A. Mydosh, and K. H. J. Buschow, *Phys. Rev. B* **31**, 4622 (1985).

⁶H. M. Rietveld, *J. Appl. Cryst.* **2**, 65 (1969).

⁷A. Herpin and P. Meriel, *J. Phys. Rad.* **22**, 337 (1961).

⁸Y. Isikawa, K. Higashi, T. Miyazaki, T. Sato, K. Sugiyama, and M. Date, in *High Field Magnetism* (North-Holland, Amsterdam, 1983), p. 101.

⁹G. E. Bacon, and J. Crangle, *Proc. R. Soc. London, Ser. A* **272**, 387 (1963).

¹⁰L. I. Vinokurova, V. G. Veselago, V. Yu. Ivanor, D. P. Rodionov, and L. I. Sagoyan, *Phys. Met. Metall.* **45**, 49 (1979); **45**, 169 (1979).

¹¹F. Gautier, in *Magnetism of Metals and Alloys*, edited by M. Cyrot (North-Holland, Amsterdam, 1982), p. 228, and references therein.

¹²T. Jo, *J. Phys. Soc. Jpn.* **50**, 2209 (1981).

¹³S. Chikazumi, *J. Magn. Magn. Mater.* **10**, 113 (1979).

¹⁴W. Bendick, H. H. Ettwig, and W. Pepperhoff, *J. Phys. F* **8**, 2525 (1978).

¹⁵A. Z. Menshikov, *J. Magn. Magn. Mater.* **10**, 205 (1979).

¹⁶D. M. Roy and D. G. Pettifor, *J. Phys. F* **7**, L183 (1977).

¹⁷O. K. Anderson, J. Madsen, U. K. Poulsen, O. Jepsen, and J. Kollar, *Physica* **86-88B**, 249 (1977).